Agent-assisted Electrokinetic treatment of Sewage Sludge: Heavy Metal Removal Effectiveness and Nutrient Content Characteristics

Agent-assisted Electrokinetic treatment of Sewage Sludge: Heavy Metal Removal Effectiveness and Nutrient Content Characteristics

Xutong Wang [a, b], Xiaoqiang Cui [a], Cheng Fang [c], Fan Yu [d], Jun'ao Zhi [c], Ondřej Mašek [b, *], Beibei Yan [a], Guanyi Chen [e, **], Zeng Dan [c]

[a] *School of Environmental Science and Engineering, Tianjin University, Tianjin 300072, China*

[b] *UK Biochar Research Centre, School of Geosciences, University of Edinburgh, Crew Building, Alexander Crum Brown Road, Edinburgh EH9 3FF, UK*

[c] *School of Science, Tibet University, Lhasa 850012, Tibet Autonomous Region, China*

[d] *Institute of Energy and Power Engineering, Zhejiang University of Technology, Hangzhou 310023, China*

[e] *School of Mechanical Engineering, Tianjin University of Commerce, Tianjin 300134, China*

Corresponding Authors:

* E-mail: ondrej.masek@ed.ac.uk (Ondřej Mašek); chengy@tjcu.edu.cn (Guanyi Chen).

Abstract

Sewage sludge (SS) is rich in nutrient elements such as phosphorus (P), nitrogen (N), and potassium (K), and therefore a candidate material for use in agriculture. But high content of heavy metals (HMs) can be a major obstacle to its further utilization. Therefore, an appropriate HM removal technology is required before its land application. In this study, an innovative biodegradable agent (citric acid, $FeCl_3$, ammonium hydroxide, Tetrasodium iminodisuccinate (IDS), and tea saponin) assisted electrokinetic treatment (EK) was performed to investigate the HM removal efficiency (R_{HMs}) and nutrient transportation. Citric acid, IDS, and $FeCl_3$-assisted EK showed a preferable average R_{HMs} (R_{ave}) reduction of 52.74−59.23%, with low energy consumption. After treatment, the content of Hg (0.51 $mg \cdot kg^{-1}$), Ni (13.23 $mg \cdot kg^{-1}$),

and Pb (26.45 mg·kg^{-1}) elements met the criteria of national risk control standard, in all cases. Following the treatment, most HMs in SS had a reduced potential to be absorbed by plants or be leached into water systems. Risk assessment indicated that the Geoaccumulation index (I_{geo}) value of HMs has decreased by 0.28−2.40, and the risk of Pb (I_{geo}=−0.74) reduced to unpolluted potential. Meanwhile, no excessive nutrient loss in SS occurred as a result of the treatment, on the contrary, there was a slight increase in P content (18.17 mg·g^{-1}). These results indicate that agent-assisted EK treatment could be an environmentally-friendly method for R_{HMs} and nutrient element recovery from SS, opening new opportunities for sustainable SS recycling and its inclusion into circular economy concepts.

Keywords: Electrokinetic treatment, Sewage sludge, Heavy metals, Nutrient analysis, Biodegradable agents

1. Introduction

In recent years, rapid economic development and urbanization have led to a massive increase in municipal wastewater production. To solve this, 15 wastewater treatment plants (WWTPs) have been set up in Lhasa by 2019, and more WWTPs have been put into Naqu, Shigatse, and other places in Tibet. The total annual SS production amount has reached up to 7.69 × 10^7 tons (water content of 80%) (Chen et al., 2021b). Although SS production is increasing sharply, Tibet's current SS treatment capacity and treatment technology are seriously inadequate. A large amount of SS was accumulated in the WWTPs, which seriously affects the normal operation of the

46 factories. The magnitude of SS production has stimulated the search for proper
47 treatment options to avoid irreversible impacts.

48 SS is rich in nutrient elements, for example, P, N, and K required for plant growth,
49 considerably higher than in many other materials, including biomass and manures
50 (Tang et al., 2022). However, SS can contain a range of harmful substances, including
51 HMs, and organic pollutants (Xia et al., 2020). More than half of HMs in wastewater
52 would be condensed in SS through bacterial absorption and mineral particle adsorption
53 (Wang et al., 2021b), resulting in relatively high concentrations. Among the HMs
54 typically found in SS, Hg, Cu, Pb, Cr, Ni, Zn, and Cd, are the main obstacle to further
55 agricultural applications of SS (Yesil et al., 2021). Notably, Cu content (121.15
56 $mg \cdot kg^{-1}$) in Tibetan SS used in this study was about 2.4 times higher than the national
57 soil environmental risk control standard value (50 $mg \cdot kg^{-1}$). Cd concentration (0.63
58 $mg \cdot kg^{-1}$) reached over 14.4 times higher than the soil background value of Tibet (0.04
59 $mg \cdot kg^{-1}$). Without proper treatment, these harmful substances would be released into
60 the environment, causing pollution and endangering public health (Zheng et al., 2020).
61 Even with moderate content of HMs in SS, bioavailable metals can accumulate in soil
62 or vegetation over time with repeated SS applications (Zheng et al., 2021). Considering
63 the fragile ecosystems in Tibet, and the many not yet fully understood potential risks
64 of HMs, both HM concentration and bioavailability should be reduced prior to
65 utilization of SS and its derived products in agricultural fields.

EK technique employs a low-level direct current that passes across SS, enabling contaminants to migrate towards anode or cathode by electrophoresis, electromigration, and electroosmosis (Zeng et al., 2021). During EK treatment, water is reduced at the cathode chamber to produce hydroxyl ions (OH^-), and water oxidation occurs in anode chamber and produces H^+ ions. Lower pH increases the R_{HMs} by dissolving the stable HMs into exchangeable forms (Zhang et al., 2020). Tang et al. (2021) reported high R_{Cu}, R_{Zn}, R_{Cr}, R_{Pb}, and R_{Ni} (~60.40%) by approaching anode EK technique by SS acidification and pH decrease. Researchers (Chen et al., 2021a; Liu et al., 2017; Tang et al., 2020; Xu et al., 2017) applied various chemicals to reduce electrolyte pH variation, which all confirmed the feasibility of EK treatment with considerable R_{HMs} (19−34%). However, these researches mainly focus on R_{HMs} of SS but ignored the further utilization potential of the EK treated SS (EKSS). Though Xu et al. (2019) claimed no excessive Na^+ and Mg^{2+} loss in EK treated soil was observed, and Kou et al. (2020) proved that C, N, and P were retained after ethylenediaminetetraacetic acid (EDTA)-acid extraction treatment of digested SS. No related research illustrated the changes of nutrient elements (N, P, and K) in EKSS or evaluated its potential for further utilization.

Besides, EK technique faces some challenges as the dissolved HMs ions are adsorbed on the SS particles and form precipitates with carbonates, hydroxides, and other compounds near the cathode in the high pH area, blocking the EK process. Recently, chemical additives were employed to break the above-mentioned obstacle

and improve R_{HMs}. Chen et al. (2021a) added Dicarboxymethyl glutamic acid (GLDA) to pretreat flue gas desulfurization-derived SS in EK treatment. Their results showed that R_{Cr} increased by 22.48% compared to the unenhanced EK process. Traditional chelating agents, including EDTA (Hanay et al., 2009), ethylenediamine disuccinic acid (EDDS), and nitrilotriacetic acid (NTA) (Song et al., 2016) were also tested to improve R_{HMs} in EK treatment by solubilizing the HMs. But, most traditional agents are non-biodegradable posing secondary pollution and potential risk to the environment. Therefore, five representative types of non-toxic and biodegradable agents, including organic acid (citric acid), alkaline (ammonium hydroxide), inorganic salt ($FeCl_3$), traditional chelation agent (IDS), and eco-friendly chelating agent (tea saponin) were chosen to enhance R_{HMs} of SS in the EK technique in this paper.

Citric acid has been used to improve the R_{HMs} by adjusting the pH value, while ammonium hydroxide could transform the stable HMs into unstable states (Suanon et al., 2016). $FeCl_3$ has been reported for HM removal as increasing the ions concentration in the SS solution and governed by the hydroxide equilibria (Moon et al., 2021). IDS is an eco-friendly chelator to replace the traditional chelating agent, which is mainly utilized as a water treatment agent for its strong chelation of HMs (Wu et al., 2015). These agents showed high potential for R_{HMs} by chemical extraction method (Ma et al., 2020; Xu et al., 2017), but few researchers combined them with EK treatment. Tea saponin is extracted from tea tree seeds with good biological activity and has an obvious effect on R_{HMs} by reducing surface tension. Although previous studies (Tang et al.,

2020; Tang et al., 2018) indicated that biosurfactants (rhamnolipid, saponin, and sophorolipid) could enhance EK treatment which improved R_{Cu}, R_{Zn}, R_{Pb}, and R_{Ni} by 23−30%, respectively, compared to the unenhanced EK treatment. But the mechanism of biosurfactants in EK treatment remains largely unknown. As different agents had varying effects on the R_{HMs}, due to their different mechanisms, this study focused on, investigation and comparison of the effectiveness of five different types of eco-friendly agents and underlying mechanisms.

In this study, Tibetan SS was treated with five agent-assisted EK treatments. The primary factors of EK process were tested, including pH, current, and energy consumption. HM concentration and its distribution were investigated to explore the mechanism of agent-assisted EK process. In addition, specific nutrient content (N, P, and K) transformation in SS during EK treatment was determined to evaluate its further utilization potential. Moreover, the environmental risk of treated SS was estimated by the I_{geo}, which is essential for the eco-environment system in Tibet. The objectives of this study were to (1) illustrate the effects of different agents on R_{HMs} and mechanism of agent-assisted EK treatment, (2) identify the nutrient element changes, and (3) determine energy consumption and environmental risk of the treatments.

2. Materials and methods

2.1 SS sample

SS was collected from Tibet Origin WWTP CO., Ltd, Tibet, with an average flow of 200,000 $m^3 \cdot d^{-1}$ that serves 1 million equivalent inhabitants. The collected SS was

the secondary treatment sediment, after further drying until no further weight loss, ground into powder, and passed through a 0.15-mm sieve.

2.2 EK experiments

EK treatment was performed in an EK reactor shown in Fig. 1. A pair of Titanium plate electrodes were placed in each electrode chamber. To avoid SS leakage into the electrode chambers, exchange membranes (CMI-7000) were attached to the plexiglass plate. EK experiments were carried out at room temperature for 120 h (Peng and Tian, 2010) at a constant voltage of 24 V, and 0.1 M KH_2PO_4 was used as the electrolytes. 400 g of dry sludge was mixed with 1.2 L deionized water (water content: 75%). EK0 was the unenhanced EK treatment using deionized water as the agent. In agent-assisted EK treatment, SS was mixed with 0.1 $mol \cdot kg^{-1}$ Citric Acid (referred to as EK1), Ammonium hydroxide (EK2), $FeCl_3$ (EK3), IDS (EK4), and tea saponin (EK5). SS was mixed with solutions for 24 h to ensure uniformity before the reaction. During the reactions, the electrolyte solution was refreshed every 24 h. The electric current was monitored every 12 h by a multimeter. After the reaction, SS samples were oven-dried, ground, and passed through a 0.15-mm. The EKSS derived from EK0−EK5 and were separately labeled as EKSS0−EKSS5.

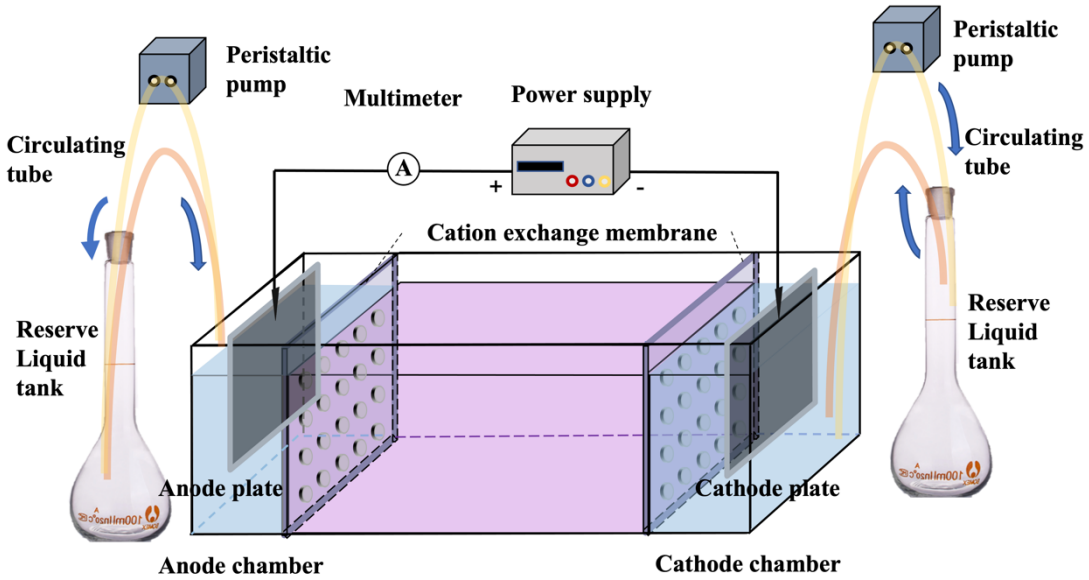

Fig. 1. Schematic of the EK reactor.

2.3 Chemical and analytical methods

2.3.1 Sludge characteristic analysis

The pH of SS was determined every 24 h by a pH meter (PHS-3C, Shanghai Metash). The compositions of cathode sediments were determined by X-ray fluorescence spectrometry (XRF, PANalytical Axios) and X-ray diffraction (XRD, D8 advance). The specific surface areas and pore size of SS were determined by N_2 isothermal adsorption-desorption behavior using a Micrometrics ASAP-2010 automated system. Scanning electron microscope (SEM, JSM-7610F) was induced to characterize the structure of SS.

2.3.2 HMs analysis

The HM concentrations in SS and EKSS were determined by an inductively coupled plasma-mass spectrophotometer (ICP-MS, iCAP Q, Thermo) after acid digestion. R and R_{ave} was calculated by Eq. (S1−S2). The sequential extraction was

161 performed using a four-step modified European Community Bureau of Reference
162 (BCR) procedure. All the measurements were performed in triplicate, and the standard
163 deviation was obtained by descriptive statistics.

164 2.3.3 Energy consumption

165 To evaluate energy efficacy, the specific energy consumption per R_{HMs} (E_u) was
166 proposed based on the cumulative energy consumption (E).

$$E = \int_0^t UI \ dt_0 \quad (1)$$

$$E_u = \frac{E_i}{R_{ave_i} \ or \ R_{HM_i}} \quad (2)$$

167 where U represents the voltage (V), I represents the electric current (A), and t stands
168 for the reaction time (h), Eu represents the energy consumption on R_{HMs} or R_{aves} for
169 each EK treatment (kWh).

170 2.3.4 Nutrient content

171 Total P (TP), Inorganic P (IP), and Organic P (OP) contents in SS and EKSS were
172 analyzed by the Standard Measurement and Testing (SMT) method, and P
173 concentration was analyzed by ascorbic acid method with visible spectrophotometer
174 (UV-6000PC, Shanghai Metash) in triplicate. TN of samples was tested by organic
175 elemental analyzer (Thermo Scientific Flash 2000). TK was determined by ICP-MS
176 after acid digestion.

177 2.4 Risk analysis

178 Geoaccumulation index (I_{geo}) was calculated by Eq. (S3) and the criteria for I_{geo} is
179 shown in Table S10.

2.5 Statistical analysis

The intensity of correlation between R to pH and current was determined by Pearson correlation coefficient. Significant differences were calculated by one-way analysis of variance (ANOVA), and a post-hoc test was determined by Waller-Duncan in SPSS 24.0.

3. Results and discussions

3.1 Effect of agents on R_{HMs}

3.1.1 R_{HMs}

HM concentrations in SS, EKSS, and control standards of pollutants for agricultural use (GB 4284−2018) are listed in Table S1. HM concentrations except for Ni and Pb in SS exceeded the limitations in the standard. All HM concentrations were much higher than the soil background in Tibet reported by the Ministry of Environmental Protection of China (Table S1). After EK treatment, Hg, Ni, and Pb met the risk control standard (GB 4284−2018). The concentration of the remaining elements (Cd, Cr, Cu, and Zn) fell below the standard value in EK1, while there were some exceptions in EK2−EK5, and none of these elements reached the risk control value in EK0. In the following discussion, the R_{HMs} were discussed in the order of HMs, and the mechanisms behind performance of the different agents in the EK treatments were analyzed.

As demonstrated in Fig. 2 and Table S2, EK0 exhibited the lowest R_{ave} among EK treatments, while only Hg obtained a high R of 70.08%. The agent-assisted EK

treatment favored R_{HMs} in various degrees, compared to EK0, the R_{ave} was enhanced from 39.33 to 59.23%. EK1 showed the best acceleration performance with higher RCr, R_{Cu}, R_{Ni}, and R_{Zn} than that in other circumstances, indicating citric acid was a promising agent. Two reasons might lead to this phenomenon: (1) more H^+ were released after mixing citric acid with SS, which boosted the HMs desorption from SS surface by competing for active adsorption sites of SS with HM ions (Tang et al., 2016); (2) functional groups (hydroxyl and carboxyl) integrated by soluble organics with HMs prevented the re-adsorption of HMs (Ma et al., 2020).

Specifically, in EK1, the R_{Cr} significantly raised from 11.98% (EK0) to 58.22% (EK1) ($F = 219.80$, $P < 0.01$). As shown in Fig. 2, the increase in R_{Cu} and R_{Zn} was less evident than Cr in EK1 compared to EK0 ($P < 0.01$). And R_{Cu} demonstrated positive correlations with Ni ($r = 0.92$, $P < 0.01$) and Zn ($r = 0.95$, $P < 0.01$), indicating that citric acid had homologous effects on the R_{Cu}, R_{Ni}, and R_{Zn} (Table S4). Unlike the results illustrated by Li et al. (2020a) where the traditional EK treatment had a much greater R_{Cu} than R_{Zn} because of the high transfer rate of Cu^{2+}. Similar R_{Cu} and R_{Zn} were obtained because the constant voltage in this study ensured each element had a strong reaction to the voltage and migrated towards the cathode. Agent-assisted EK had significant ($F = 19.69$, $P < 0.01$) enhancement effects on R_{Ni} from 21.93% (SS) to 55.73% (EK1). The R_{Ni} in Peng and Tian (2010)'s research (34%) was lower than in this study (55.73%), where adopted citric acid as electrolyte to enhance the R_{HMs}. This implied that citric acid showed better R_{Ni} by forming mobile complexes with HM ions in SS than the effect

of controlling electrolyte circulation and pH. Notably, R_{Ni} implied strong correlations with R_{Pb} ($r = 0.96$, $P < 0.01$) and R_{Zn} ($r = 0.83$, $P < 0.05$).

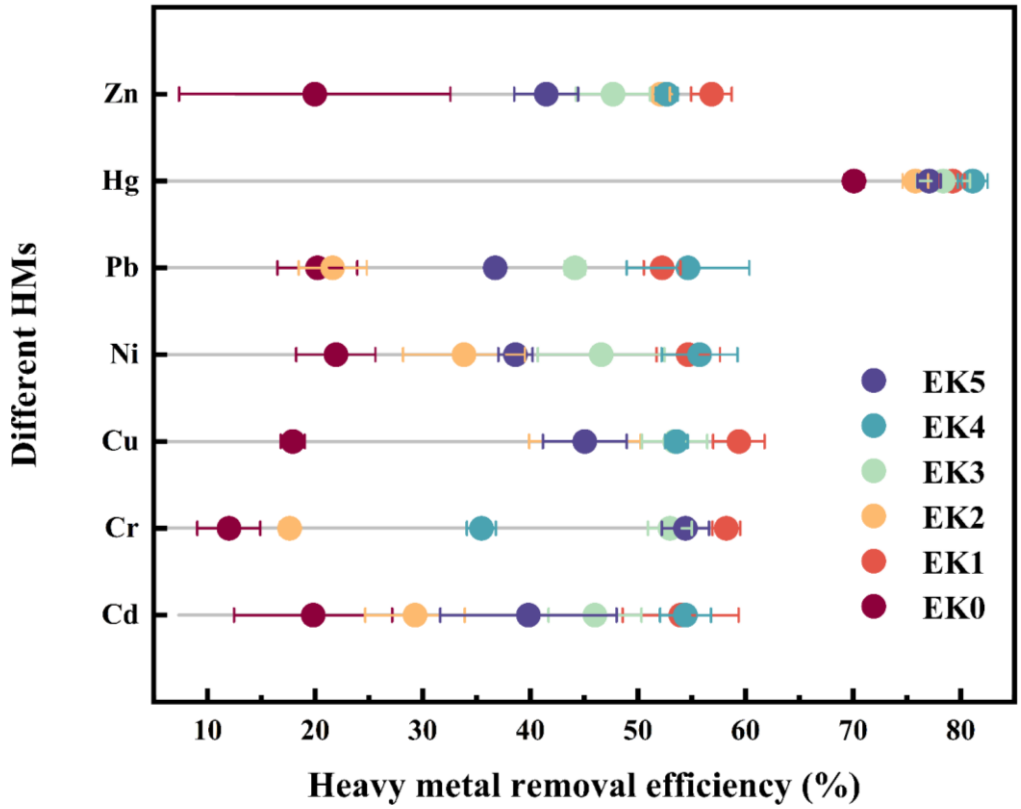

Fig. 2. R_{HMs} of different EK treatments (%).

Error bars represent standard deviation observed for triplicate experiments (smaller than symbol if not shown).

The R_{Hg} was the highest in all treatments and showed minor differences in agent-assisted treatments and the unenhanced EK (Fig. 2). The R_{Hg} in EK0 was similar to the highest R_{Hg} (70.93%) in Falciglia et al. (2016) 's study. As shown in Table S4, Hg exhibited strong positive correlation with Ni, Pb, and Zn ($P < 0.05$). Indicating desorption of these metal ions from SS was synergistically strengthened by adding agents, which led to higher R via acceleration of electromigration. R_{Cd} had significantly

234 ($F = 11.76$, $P < 0.01$) improved from 19.81% (EK0) to 54.42% (EK4). Cd showed close
235 positive correlation with Cu ($r = 0.90$, $P < 0.05$), Hg ($r = 0.95$, $P < 0.01$), Ni ($r = 0.99$,
236 $P < 0.01$), and Pb ($r = 0.98$, $P < 0.01$). It indicated that the R of these elements showed
237 similar responses with the combination of chelating effect and EK treatment. And
238 agents significantly ($F = 43.90$, $P < 0.01$) stimulated R_{Pb} from 20.21% (SS) to 54.65%
239 (EK4). Therefore, IDS was the second effective agent for R_{HMs} after citric acid, as it
240 showed the highest R_{Hg}, R_{Cd}, and R_{Pb}.

241 Metals extraction by citric acid and IDS was based on the affinity of the organic
242 ligand for HMs and the extent of complexation between polydentate HMs and organic
243 ligands, which were determined by stability and amount of metal-binding functional
244 groups on the chelator (Kołodyńska et al., 2009). In EK4, R varied a lot on each HMs
245 because of the different responses to IDS. Stability constants (S) of IDS on each HM
246 complexes was with the order of S_{Hg} (14.9)> S_{Cu} (13.1) > S_{Ni} (12.2) > S_{Pb} (11.0) > S_{Zn}
247 (10.8) > S_{Cr} (9.6) > S_{Cd} (8.4) (Wu et al., 2015). While in this study, R reduced with the
248 sequence of Hg> Ni> Pb> Cd> Cu> Zn> Cr, the extraction of HMs from SS was closely
249 related to the sequence of stability constants with slight modification. Given the
250 response to the agent, the formation of compounds between metals and hydroxyl groups
251 varied from each element (Raheem et al., 2018).

252 The R_{ave} reduced in the order of EK1> EK4> EK3> EK5> EK2> EK0 (Fig. 2). R_{Cd},
253 R_{Ni}, R_{Pb}, and R_{Zn} showed minor differences in EK3. In EK5, R_{Cr} was higher than that in
254 EK2–EK4, owing to the reduction of surface tension in metals. The surfactant micelles

255 in tea saponin provided hydrogen ions that promoted the migration and biodegradation
256 of HMs during the process. And carbonyl in tea saponin indicated its strong chelating
257 capability with HMs. Markedly, the R_{Cr} was not correlated with any other element, and
258 hence the mechanism of the agent-assisted EK remained unknown. Agents could
259 destroy the compounds in HMs (Tang et al., 2017), and the fractions of HMs might be
260 vastly changed after agent-assisted EK treatments. To illustrate the role of agents on
261 EK treatment, the bioavailability, and toxicity of HMs in EKSS, more detailed
262 discussions focusing on the speciation of the HMs are needed.

263 3.1.2 HMs speciation variations in EKSS

264 Applying different agents resulted in noticeable differences in the speciation of
265 different HMs (Fig. 3). The sum of acid-soluble and reducible proportion of Cu was
266 49.02% in SS, it reduced to 35.6−42.1% in EK1−EK3, and EK5. The oxidizable
267 fraction accounted for the highest ratio of the four fractions in all agent-assisted EK
268 treatments, which indicated EKSS were relatively stable and would liberate the soluble
269 metals only in oxidizing conditions (Raheem et al., 2018). The oxidizable fraction of
270 EK1 was up to 57.9%, and approximately 10.5% of the reducible fraction was
271 converted to the oxidizable fraction. Implying that the citric acid accelerated the
272 unstable states of HMs transfer into stable status. In EK2−EK5, the oxidizable fractions
273 fluctuated by 36.4% to 47.0%, therefore, main distributions of Cu have not changed in
274 the rest of agent-assisted EK treatment, in agreement with Wang et al. (2021a)'s study.

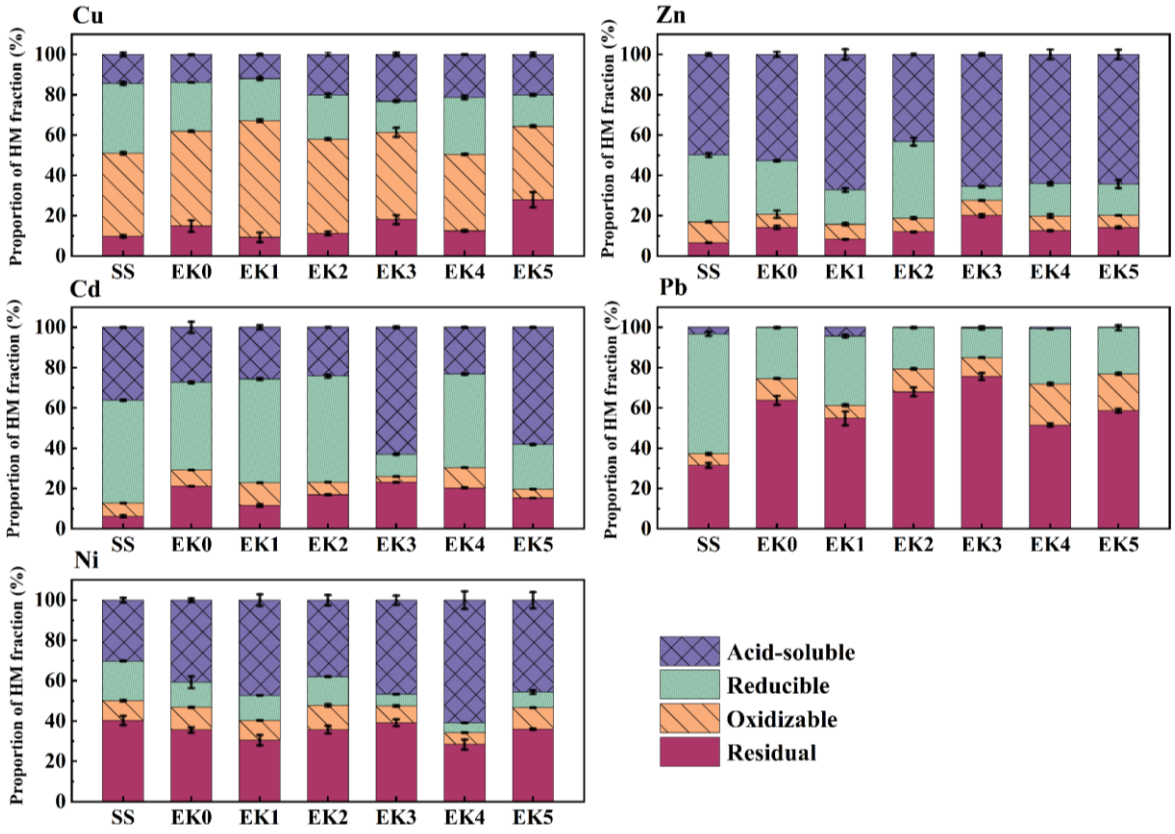

Fig. 3. Distribution of HMs in SS and EKSS (120 h).

Error bars represent standard deviation observed for triplicate experiments (smaller than symbol if not shown).

The acid-soluble and reducible fractions of Zn accounted for up to 83.1% of Zn in SS, resulting in a high environmental risk used on land (Dai et al., 2019). The residual fraction accounted for 6.6% in SS, increased to 20.1% in EK3. The residual fraction was related to the crystalline mineral in SS, and agents, especially $FeCl_3$ showed the ability to dissolve the silicate and mineral matter. The acid-soluble fraction was negatively correlated ($r = -0.93$, $P < 0.01$) with the reducible Zn fraction (Table S4). The acid-soluble fraction increased after EK treatment, except for EK2, as reducible fractions were partly converted into acid-soluble fractions. Tang et al. (2021) claimed

that the acid-soluble fraction of Zn was easier to remove in EK treatment, therefore reaction time might be insufficient for R_{Zn} in this study. Hanay et al. (2009) also clarified the unchangeable Zn fractions in agent-assisted EK treatment because of the insufficient concentration of the washing solution.

The acid-soluble and reducible fractions of Cd in SS were in excess of 87.20%, indicating an easy to extract state. The residual fraction accounted for 6.2% and increased to 23.2% after EK treatment. The acid-soluble fraction of Cd indicated a significant negative correlation with the reducible fraction ($r = -0.98$, $P < 0.01$). The acid-soluble fractions increased from 36.2% to 63.0% (EK3) and 58.1% (EK5), but R_{Cd} in EK3 and EK5 were lower than that in EK1 and EK4. The chelation of tea saponin led to the competition of HM ions with organic matters in SS, enhancing reducible fraction conversion to acid-soluble states. In comparison with other agents, $FeCl_3$ likely promoted the transformation of HMs from stable to unstable states. And the oxidizable fraction indicated negative correlation with acid-soluble ($r = -0.84$, $P < 0.05$) fraction, while showing positive correlation ($r = 0.83$, $P < 0.05$) with reducible fraction. This phenomenon was obvious in EK1, and similar results were obtained in Chen et al. (2021a)'s study. The chelation of citric acid caused the competition of HMs ions with organic matters in SS, enhancing the conversion of oxidizable fractions to easily removable states, thereby facilitating R_{Cu}.

Residual and reducible fractions were the key forms of Pb and accounted for 31.5% and 59.5%, respectively. The proportion of acid-soluble fraction of Ni was relatively

low in SS and decreased below 1% of the total Ni in most of the EK treatments, which implied limited potential to be absorbed by plants or to be leached into water systems. In addition, the residual fractions of Ni dramatically increased in all EK treatments, rising to 63.7% (EK1) and 75.6% (EK3) correspondingly, their R_{Pb} was higher than in other EK treatments. Indicating that HMs likely formed more stable complexes with the citric acid functional groups and were likely to be extracted in citric acid-assisted EK treatment (Ma et al., 2020).

The acid-soluble and reducible fractions presented similar proportion with oxidizable and residual fractions of Ni, the high ratio of stable fractions retarded R_{Ni} from SS. After EK treatment, the stable fractions of Ni changed to easy to extract states, which was also observed in a study by Liu et al. (2017). Indicating that if an appropriate treatment process is followed by EK treatment, HMs would be more effectively removed, and the coupling treated EKSS would be more suitable for land utilization (Yuan and Weng, 2006). The oxidizable fraction of Ni indicated negative correlation with acid-soluble ($r = -0.95$, $P < 0.01$), while showed positive correlation ($r = 0.85$, $P < 0.05$) with reducible fraction. Therefore, agents showed synergetic effect on the removal of oxidizable and reducible fractions with SS.

3.1.3 Impact of agents on electric current and sludge pH

R_{HMs} is closely related to the sludge pH and electric current (Fig. 4). Overall, EK3 showed the lowest pH values (5.50 to 2.35), while other treatments fluctuated with the minimum pH value of 3.36 to 3.73, except for EK2 (4.44). As shown in Eq. (3), H^+ ions

were continuously generated along with the release of charges due to water electrolysis in the anode chamber and migrated into the reaction chamber. In EK3, Fe^{3+} in $FeCl_3$ converted to Fe^{2+} with the ions in the reaction chamber, which reduced the pH value by accumulating the H^+ ions. A low pH value could encourage the transformation and dissolution of HMs fractions (Cherifi et al., 2016), suggesting that adding $FeCl_3$ improved the R_{HMs} by reducing the reaction pH. Conversely, ammonia might bind with the H^+ in SS solution and generate more OH^- by inducing the electrolysis of water Eq. (4); OH^- enrichment resulted in a higher pH value in EK2.

$$2H_2O \longrightarrow O_2 + 4H^+ + 4e^- \quad (3)$$

$$2H_2O + 2e^- \longrightarrow H_2 + 2OH^- \quad (4)$$

Adding citric acid, IDS, and tea saponin were ineffective in reducing the pH value compared to EK0. The buffer solution KH_2PO_4 in the electrode chamber helped maintain the pH value in the cathode and anode chambers. Besides, citric acid contains three carboxyl function groups (−COOH), increasing its buffering capacity and helping maintain an acidic pH value from 3 to 6. Nevertheless, the carbonates in the natural sediment of citric acid prevented the migration of hydrogen ions from the anode towards the cathode (Song et al., 2016). IDS is a pentadentate complexing agent that forms octahedral chelates with many metal ions. The reaction with metals varied with the pH and concentration of the solution, four possible stereoisomers of IDS could react with the metal ions with the following reversible reaction:

$$M^m + IDS^n \leftrightarrows [\mathrm{M(IDS)}]^{(n-m)^-} \quad (5)$$

$$H_3IDS^- + H^+ \leftrightarrows H_4IDS \quad (6)$$

$$H_2IDS^{2-} + H^+ \leftrightarrows H_3IDS^- \quad (7)$$

$$HIDS^{3-} + H^+ \leftrightarrows H_2IDS^{2-} \quad (8)$$

$$IDS^{4-} + H^+ \leftrightarrows HIDS^{3-} \quad (9)$$

The pH value of EK4 was around 6.0 to 4.0, and the acid condition was suitable for Ni removal (Ma et al., 2020). The pH value of EK5 was slightly lower than EK0 because tea saponin is a non-ionic surface-active agent, and its functional group could change the physicochemical properties of SS. The aqueous solubility and mobility were strengthened by their asymmetric structure. The hydrogen bonding and electrostatic forces between HMs and tea saponin also accelerated *R* (Rahman et al., 2022). As for EK1, adding citric acid reduced the pH value of SS, owing to the complexes formed by citric acid and HMs promoted the HMs mobility through electro-migration and electro-osmosis.

The pH value showed strongly positive correlation with the reducible fraction of Zn ($r = 0.88$, $P < 0.05$) and Cd ($r = 0.89$, $P < 0.05$). It can be inferred that high pH value and the high reducible fraction proportion of Cd, and Zn hindered its extraction rate. As mentioned in 3.1.1, R_{Cd} and R_{Zn} demonstrated positive correlation with R_{Cu}. Still, the pH did not display any correlations with fractions of Cu. This was due to the preferable reduction of reducible fraction proportions after EK treatments. And acid-soluble fraction of Cd exhibited significant negative correlation with the pH value ($r = -0.82$, $P < 0.05$). This illustrated that the acid-soluble extraction would be accelerated by reducing the pH, this was contrary to Chilian et al. (2022) 's study where the removal of acid-soluble fraction was strengthened by the increase of pH values. This was mainly

because the response to pH was different by elements; the extraction of Al, Fe, and Cl had better extraction potential under alkaline solutions rather than Cd element.

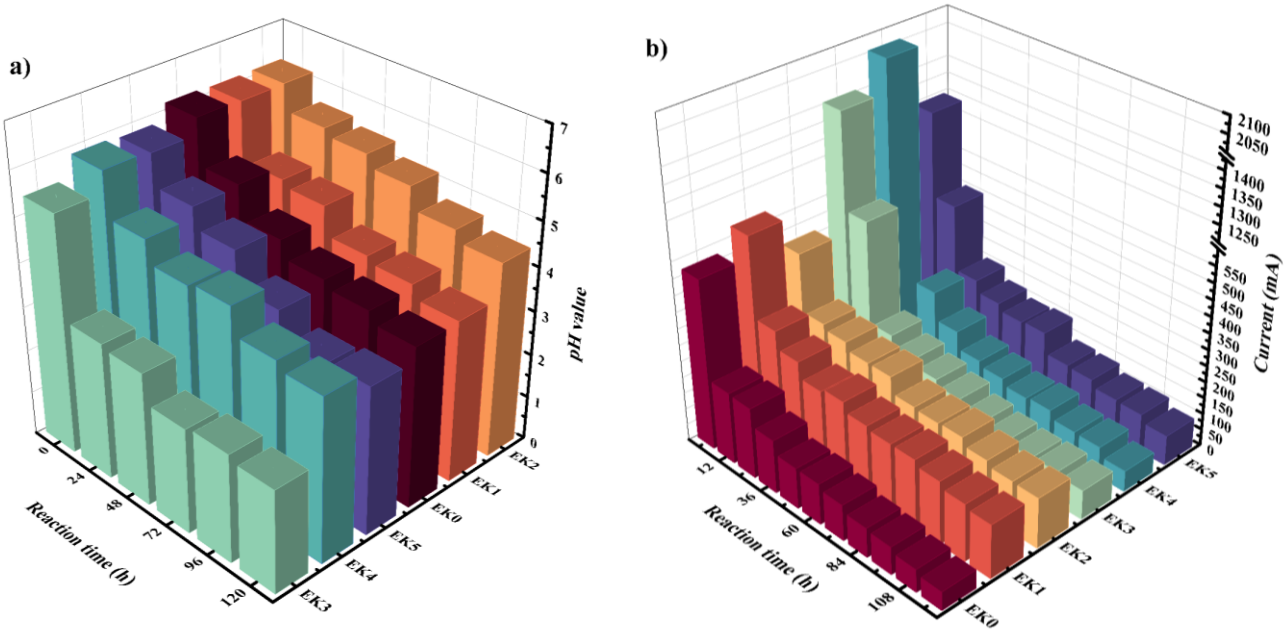

Fig. 4. a) Sludge pH variation and b) electric current variation during EK process.

As the EK process was under a constant voltage, electric current variations (Fig. 4b) reflect conductivity and ion exchanges (Tang et al., 2018). The initial current reached the maximum value at the beginning of the process, then rapidly dropped in the first 24 h, and gradually declined until the end of the treatment. EK0 was with the lowest current on average compared with other treatments. Notably, the initial current of EK0 was 522 mA, which was much higher than the previous study (~100 mA) (Tang et al., 2017).

EK4 had the highest initial current (2059 mA), approximately four times higher than EK0. This was mainly because IDS is rich in Na^+ ions and was initially active in the EK treatment, and could rapidly migrate under the electric field. High currents accelerated electrophoresis and electroosmosis and allowed HM removal by frequent

migration of charged ions (Chen et al., 2021a). The initial current of EK3 was high, but it dramatically dropped after 24 h, and the average current value after 24 h was closed to EK0. Therefore, adding $FeCl_3$ increased the current for a short duration, but was unable to improve the current in the subsequent reaction, as it may accumulate during the treatment. Similarly, EK1 and EK2 reached around 400−500 mA initially but dropped steadily during the rest of the process. The average current value of the EK1 from 24 h to 120 h was the highest in EK treatments and ended at 164 mA, which was higher than the maximum value in Tang et al. (2018) 's study. This might attribute to the regular refreshment of the electrolyte solutions in this study. Electrolytes played a key role in maintaining the stability of the current, as OH^- and other substances in the cathode would hinder the ion's migration (Xu et al., 2022). The current value of EK5 increased slightly during 48−60 h; this variation indicated a relatively stable process that occurred with the synergistic effect of tea saponin and SS. The current indicated significantly positive correlation with acid-soluble fraction of Ni ($r = 0.883$, $P < 0.05$), and negative correlation with oxidizable fraction of Ni ($r = -0.842$, $P < 0.05$). Therefore, high current could enhance the unstable fractions of Ni into easy-extraction state, and promote the R_{Ni}.

In summary, different agents had their unique functions on R_{HMs} and fraction transformation. As weak organic acid, more H^+ ions were released after adding citric acid, and its hydroxyl and carboxyl prevented the re-adsorption of HMs, therefore highest R_{Cr}, R_{Cu}, and R_{Zn} were observed. HMs tended to be converted into a more stable

state with ammonium hydroxide. Especially, Pb is more sensitive to the alkaline environment and could be slowly dissolved in ammonium hydroxide. The relatively low R_{HMs} in EK2 were attributed to the high pH values during the treatment. While Fe^{3+} in $FeCl_3$ converts to Fe^{2+} with the ions during the treatment, which reduced the pH value by accumulating the H^+ ions. A low pH value could encourage the transformation and dissolution of HM fractions, therefore the R_{ave} of EK3 was relatively high (52.74%). IDS could form octahedral chelates with many HM ions, but its stability was sensitive to the pH values. HMs showed different responses to the affinity of organic ligand, and highest R_{Cd}, R_{Hg}, $R_{Ni,}$ and R_{Pb} were reached in EK4. The surfactant micelles in tea saponin accelerated the migration and biodegradation of HMs, and carbonyl groups had strong chelating capability with HMs. Adding tea saponin enhanced reducible fraction conversion to acid-soluble states by the competition of HM ions with organic matters in SS.

3.2 Characterization of SS and EKSS

3.2.1 Properties of SS and EKSS

The specific morphology and surface area of SS and EKSS were characterized by SEM (Fig. S1) and BET (Table S8). SS had a relatively smooth surface, and hardly any pores could be seen. SS and EKSS were basically in granular form, but the particle size of EKSS was narrowed compared to SS. A few pores could be seen in EKSS with random distribution, and some irregular particles were attached to the surface. This may be due to the pH changes during EK treatment and the removal of metals from SS. The

BET results showed that the specific surface area of EKSS reduced to varying degrees after EK treatment, dropping from 42.58 $m^2 \cdot g^{-1}$ (SS) to 8.95 $m^2 \cdot g^{-1}$ (EKSS2). This reduction was consistent with previous study (Liu et al., 2020) and was likely due to the loss of surface charge. Accordingly, the pore size increased in EKSS, this could point to the adsorption of HMs degradation products on the SS surface, and the collapse of mesopores to macropores. The microscopic morphological changes of EKSS varied under different agents, but EK treatment failed to show positive changes in the morphology of SS.

3.2.2 Nutrient analysis of SS and EKSS

Fig. 5 showed that there was no excessive nutrient (TP, TK, and TN) loss in EKSS compared to SS. TP content of EKSS indicated a slight increase compared to SS, which was in agreement with other published research (13.56-20.40 $mg \cdot g^{-1}$) (Liu et al., 2021; Wang et al., 2017), but lower than that in the activated sludge (32.50 $mg \cdot g^{-1}$) (Staal et al., 2019) and anaerobically digested SS (33.60 $mg \cdot g^{-1}$) (Huang and Tang, 2015), and much higher than the wetland biomass (TP=7.58 $mg \cdot g^{-1}$) (Cui et al., 2019), wheat straw (TP=1.12 $mg \cdot g^{-1}$) (Xu et al., 2016). This increase can mainly be ascribed to the addition of KH_2PO_4 solution in electrolytes, which may introduce P to the feedstock by electromigration and electroosmosis process. Besides, the pH value dropped from 6.2 (SS) to 2.34 (EKSS3), this was consistent with the opposite relationships between pH gradient and TP contents found by Temporetti et al. (2019).

After EK treatment, the IP content increased from 9.54 $mg \cdot g^{-1}$ (SS) to 13.54 (EKSS2), and OP had partially converted to IP. IP usually originated from chemical phosphorus removal and the raw wastewater in SS, while OP was usually derived from the metabolites and assimilation of microorganisms (Yu et al., 2021). The microbial intracellular phosphorus might react with metal ions in SS under the constant voltage. This led to the release of the microbial intracellular phosphorus, meanwhile converting polyphosphate, pyrophosphate, and organic phosphorus into orthophosphate (Zhang et al., 2019), which was the main content of IP. Moreover, the reclamation of IP was relevant to the pH value of SS. EKSS2 had the highest pH value which resulted in the highest IP content in the agent-assisted EK treatments. The tendency was consistent with Yan et al. (2021)'s study that higher pH facilitated more IP release. Ping et al. (2020) found that the citrate agent could enhance the release of P by increasing IP. And Li et al. (2020b) claimed that $FeCl_3$ could fix the dissolved phosphate from apatite phosphorus in SS at the pH of 2.5, which was consistent with EK3 the pH was around 2.5 during 72−120 h. Therefore, TP concentration in SS was well preserved during EK treatment and was easy to utilize subsequently.

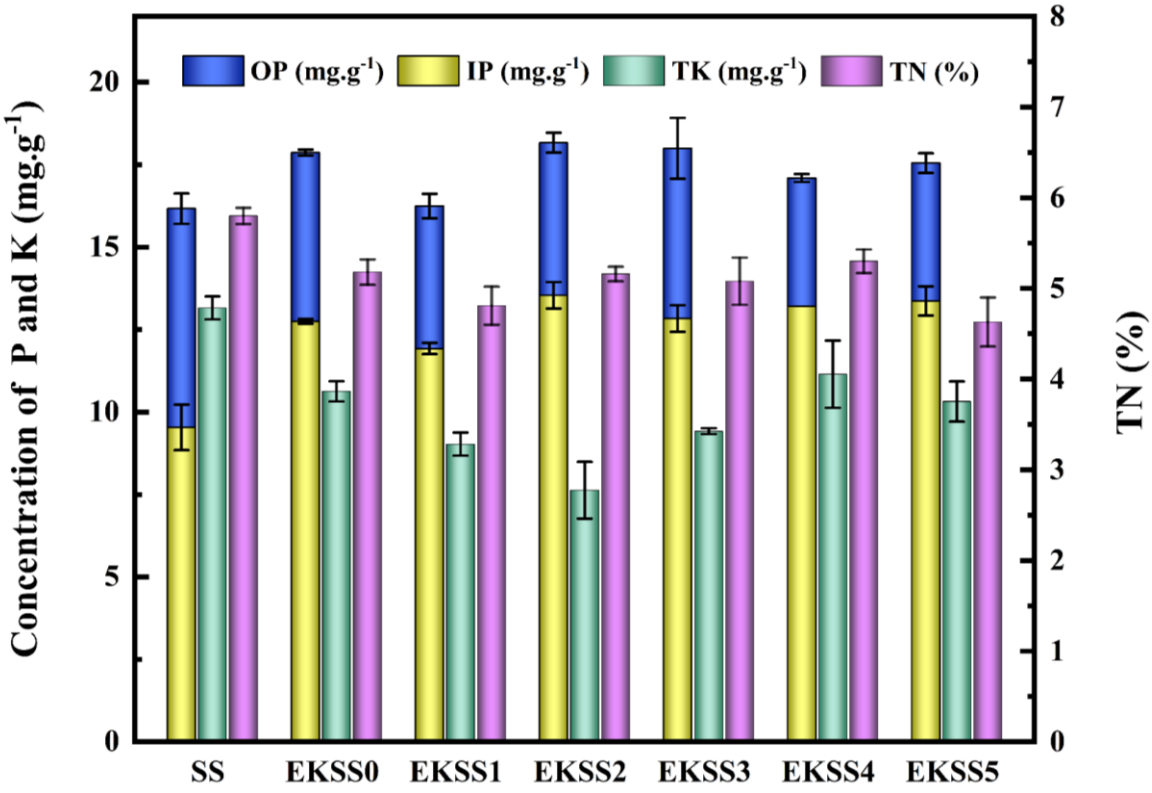

458

459 **Fig. 5**. Nutrient concentration (TP, TK, and TN) in SS and EKSS.

460 Error bars represent standard deviation observed for triplicate experiments.

461 During EK process, K^+ was extracted from SS together with HMs. TK content was
462 reduced to 7.63±0.86 mg·g^{-1} (EKSS2) and 11.15±1.02 mg·g^{-1} (EKSS4), compared
463 with 13.16±0.35 mg·g^{-1} in SS. Despite the mobility, K^+ ions may not electrodeposit
464 because of the lower reduction potential compared with HMs. Gao et al. (2022) also
465 observed the stability of K^+ and Na^+ cations and making it difficult to precipitate in the
466 electrolyte during EK treatment. The reduction was also attributed to adding alkaline
467 substances in EK, which accelerated the formation of NH_4^+ and reduced the K content.
468 Notably, the TK content of EKSS was higher than that in most of the biomass, for
469 example, it was 5 times higher than that in sawdust (2.09 mg·g^{-1}) (Wang et al., 2016),
470 and slightly higher than that in biogas residues (8.46 mg·g^{-1}), maize silage (7.31 mg·g^{-1})

471 (Wu et al., 2021b), and the pig manure (11.80 mg·g^{-1}) (Wang et al., 2016). Besides,
472 TN concentration in SS was around 5% and with minor fluctuations after EK treatment.
473 In summary, the EKSS was rich in nutrient elements with a slight reduction of TK and
474 TN content compared to SS, and no P was lost during EK treatment. The mass fraction
475 of total nutrient (TN+TK+TP) ranged from 54.46 to 60.48% which reached the national
476 standard index (5%) of organic fertilizer (NY525-2012).

477 3.3 Energy consumption and metal recycling assessment

478 As shown in Fig. 6a, E gradually increased as time elapsed. The greater E_4 and E_1
479 were consistent with their higher current. The trends were in agreement with previous
480 research (Ryu et al., 2011) showing that the energy consumption had a positive
481 correlation with current under the constant voltage gradient. E_0 was only half of E_4 and
482 E_1 because the electric conductivity of deionized water was relatively low, thus adding
483 agents improved electric conductivity of SS solution (Liu et al., 2017). Moreover,
484 adding agents accelerated the electromigration of metal ions by strengthening
485 desorption of metal ions. E_0 was similar to that reported by Song et al. (2016), but E_0–E_5
486 was lower than that of Cherifi et al. (2016). This was attributed to the fact that the
487 required E was directly related to the processing time and SS composition.

488 To evaluate energy efficacy, E_u was proposed to calculate the specific energy
489 consumption per HM removal. Lower value of E_u indicated higher energy efficacy. The
490 highest R_{ave} (59.23%) and lowest E_u (1.09 kWh) were obtained in EK1. This was
491 consistent that the lowest E_u of Ni, Cu, and Cd was achieved in EK1. Relatively low

energy consumption of 445.34 Wh·g^{-1} was obtained in previous citric acid intervening EK study (Wu et al., 2021a), with R_{Cr} of 21.62%. This might be due to the voltage gradient (1 V·cm^{-1}) was lower than this study (1.6 V·cm^{-1}). The lowest E_u of Zn was obtained in EK3 because the lowest pH value in EK3 strengthened the extraction of Zn. Besides, the lowest E_u of Hg was obtained in EK0. Because EK0 showed relatively high R_{Hg}, and the inconspicuous increase of R_{Hg} in the agent-assisted EK treatment compared to EK0. This optimal E_u (1.09−1.77 kWh) with a high R_{HMs} was more than an order of magnitude lower than that in GLDA-assisted EK treatment (Chen et al., 2021a) (10.01 kWh). Therefore, citric acid in EK1 could improve the R_{HMs} with low energy consumption.

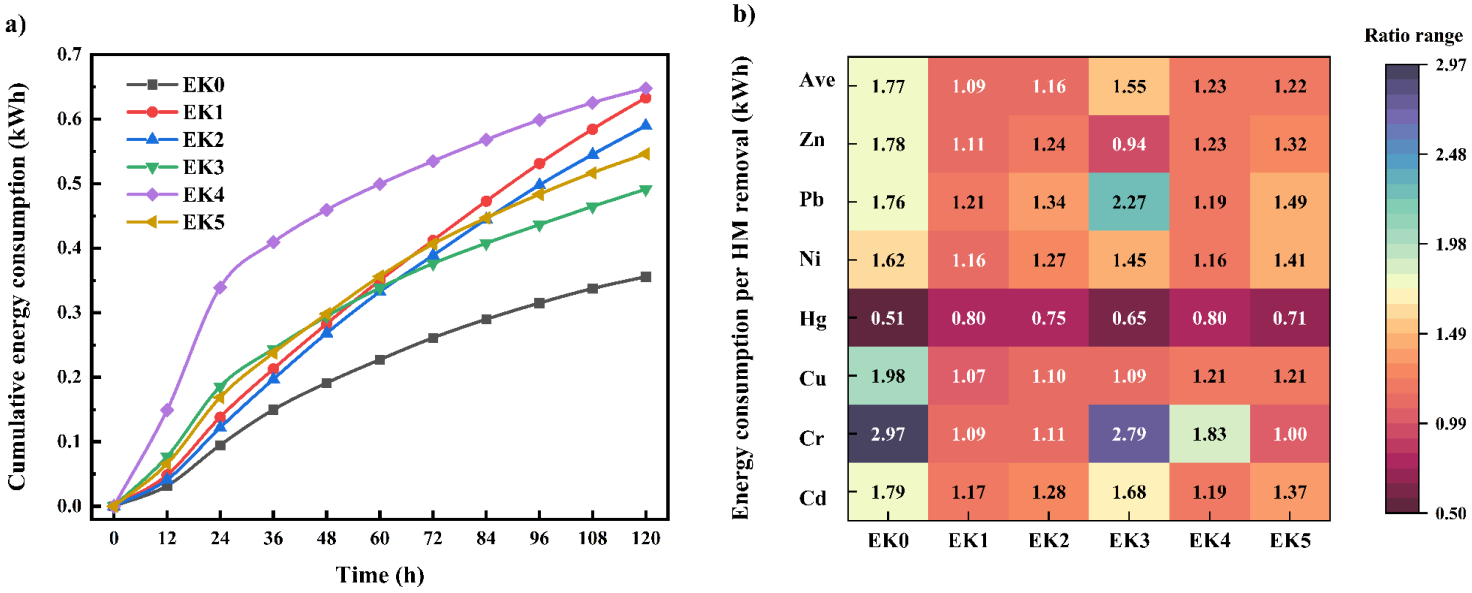

Fig. 6. a) E and b) E_u of different EK processes.

With electrophoresis and electroosmosis, sediments were accumulated as the HMs transformed from SS to the cathode chamber. To access the recycling potential of the elements, sediments from the cathode were characterized by XRF (Table S9) and XRD

506 (Fig. S2). Sediments mainly contained metal elements of Ca/K/Mg/Fe/Mn, a trace
507 amount of Si/Al, a large amount of P, and S, Cl with limited amounts. Compared with
508 SS, the proportion of P (54.83%) and K (19.67%) was higher in the sediments. This
509 was mainly due to the utilization of the buffering solution of KH_2PO_4. Ca content
510 increased from 8.81% (SS) to 27.52% (EK2), and Mg rose from 1.93% (SS) to 23.07%
511 (EK5), indicating that a large amount of Ca^{2+} and Mg^{2+} has migrated from SS to the
512 cathode chamber. Thus, recycling Ca/Mg/K/P from sediments is attemptable. Other
513 nutrient elements, such as N and Na, were saved in EKSS, which consisted of results
514 in 3.2.2. Cr only existed in the sediments of EK1 and EK4, which indicated the two EK
515 treatments had R_{Cr}. And most HMs were imperceptible as the relatively low proportion
516 in SS. XRD results showed that no secondary toxic product was generated in sediments.
517 The presence of K_2CO_3, P_2O_5, $CaHPO_4(H_2O)_2$, and ZnO in sediments were invisible in
518 SS, which was consistent with the XRF result that the high contents of Ca^{2+} and K^+ in
519 the sediments compared with SS.

520 3.4 Risk, economic assessment, and application analysis

521 I_{geo} (Fig. 7) was mainly used to estimate the contamination risk of SS and EKSS
522 for each HMs independently. I_{geo} value of SS for metals has decreased by 0.28−2.40
523 after EK treatment compared to SS. The I_{geo} values of EKSS1, EKSS2, EKSS4, and
524 EKSS5 for Pb were <0, which indicated their uncontaminated potential. SS was
525 identified as heavily contaminated levels for Cu, Cd, and Zn and fell in the moderately-
526 heavily polluted range with few exceptions. The risk level of EKSS1, EKSS2, and

EKSS5 for Cr reduced to a moderately contaminated level. SS had a moderately contaminated level for Ni and adjusted to unpolluted- moderately polluted level in EKSS. Chen et al. (2021a) noted that SS after EK treatment decreased to free of pollution levels for Cu, Zn, Ni, and Pb. However, the R_{ave} of Zn and Ni in this study was higher than that in Chen et al. (2021a)'s research, and similar R_{Cu} was observed. The reason for the difference in I_{geo} values was the relatively low HM contents in the background soil of Tibet. The I_{geo} values in SS for Hg were higher than 6 which had an "extremely contaminated" class. The values reduced to 3.70−4.36 after agent-assisted EK treatments. Hg concentration in EKSS0−EKSS5 was lower than the national risk control standards, but the I_{geo} value indicated SS had a heavily or heavily to extremely contaminated level. This may be due to the low content in the background, and the strict limitations attributed to health and agricultural considerations. The contamination level of treated SS for Hg was also reported as extremely polluted in Chen et al. (2021a)'s study. As R_{Hg} was up to 70.08−81.11% in EK treatments, some more targeted treatment, for example, coupling with post pyrolysis is suggested to further reduce the risk of Hg before direct utilization in agricultural fields.

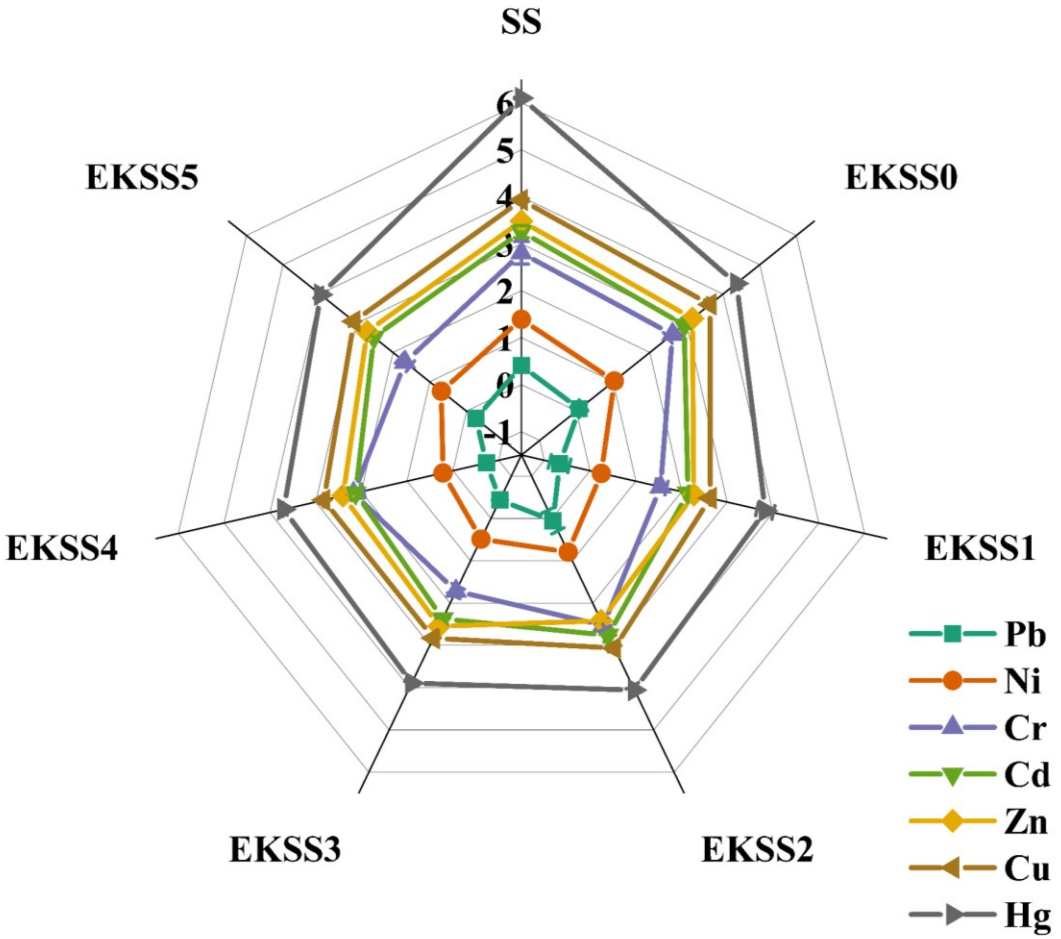

543

544 **Fig. 7**. I_{geo} of SS and EKSS.

545 Error bars represent standard deviation observed for triplicate experiments (smaller than symbol if not

546 shown).

547 The economic analysis indicated that 89.48 $\$\cdot t^{-1}$ was needed for disposing of SS

548 by EK0 (Table S11), which is in agreement with Zeng et al. (2021) who estimated the

549 costs of the EK process to be 100 $\$\cdot t^{-1}$. The cost of EK1−EK5 increased to

550 117.69−150.20 $\$\cdot t^{-1}$ due to the addition of agents. EK3 was the most economical one,

551 because of the low E and low price of $FeCl_3$. The treatment cost was cheaper than the

552 landfilling cost of SS (165–245 $\$\cdot t^{-1}$) (Zeng et al., 2021). But a more competitive cost

553 (40−50 $\$\cdot m^{-2}$) (Liu et al., 2018) was found for disposing of sediment and soil

554 remediation by EK treatment, thus further investigation on parameters affecting costs
555 is needed to improve economic feasibility.

556 Agent-assisted EK treatment showed high potential for field application, according
557 to I_{geo}, the HMs pollution risks have decreased by 0.28−2.40 after EK treatment. From
558 the perspective of R_{HMs}, Hg, Ni, and Pb met the risk control standard, and the rest HM
559 concentrations have been greatly reduced compared to SS. Meanwhile, no excessive
560 nutrient loss was observed in EKSS compared to SS. However, the economic feasibility
561 and the low ion migration speed in SS may limit the field application of EK (Xu et al.,
562 2019). Further optimization of the EK system could enhance its scalability.

563 **4. Conclusions**

564 This work highlighted that EK treatment does not result in excessive nutrient loss
565 (N, P, and K), which for the first time provided insights on further utilization potential
566 of the EKSS. Non-toxic and biodegradable agents including citric acid, IDS, and $FeCl_3$
567 showed promise as chelating agents for enhancing R_{HMs}. This significantly improved
568 R_{ave} by 26.76−33.25% and reduced pollution risk (I_{geo}) by 0.84−2.40. The R_{Pb}> 70%
569 reached in this work exceeded the average R_{Pb} of 50% in the references. Most HMs in
570 EKSS showed a lower potential to be absorbed by plants or be leached into water
571 systems. The effectiveness and mechanism of adding representative types of agents in
572 EK treatment were clarified.

573 This work provides evidence that agent-assisted EK treatment can be an
574 environmentally friendly modification method for HM removal from SS, while

retaining its nutrient content, making it a suitable amendment for use in agriculture in line with circular economy objectives. Future investigation is warranted to determine the effects of agent-assisted EK treatment on nutrient speciation transformation in SS, and its further utilization. Further optimization of the EK system is needed to enhance its scalability and reduce costs.

Acknowledgments

This work was financially supported by the National Natural Science Foundation of China (No. 51878557, No. 52160026), and National Key Research and Development Program of China (No.2019YFC1904101). We acknowledge Dr. Anjali Jayakumar for proof-reading. Xutong Wang acknowledges the supported by China Scholarship Council.

References

Chen, G., Han, K., Liu, C. and Yan, B., 2021a. Quantitative research on heavy metal removal of flue gas desulfurization-derived wastewater sludge by electrokinetic treatment. J Hazard Mater 414, 125561.

Chen, G., Zhang, R., Guo, X., Wu, W., Guo, Q., Zhang, Y. and Yan, B., 2021b. Comparative evaluation on municipal sewage sludge utilization processes for sustainable management in Tibet. Sci Total Environ 765, 142676.

Cherifi, M., Boutemine, N., Laefer, D.F. and Hazourli, S., 2016. Effect of sludge pH and treatment time on the electrokinetic removal of aluminum from water potabilization treatment sludge. Comptes Rendus Chimie 19(4), 511-516.

Chilian, A., Bancuta, O.-R., Bancuta, I., Popescu, I.V., Irina Gheboianu, A., Tănase, N.-M., Tuican, M., Zaharia, M. and Zinicovscaia, I., 2022. Extraction of heavy metals and phosphorus from sewage sludge with elimination of antibiotics and biological risks. Chem Eng J 437, 135298.

Cui, X., Yang, X., Sheng, K., He, Z. and Chen, G., 2019. Transformation of Phosphorus in Wetland Biomass during Pyrolysis and Hydrothermal Treatment. ACS Sustain Chem Eng 7(19), 16520-16528.

Dai, Q., Ma, L., Ren, N., Ning, P., Guo, Z. and Xie, L., 2019. Research on the variations of organics and heavy metals in municipal sludge with additive acetic acid and modified phosphogypsum. Water Res 155, 42-55.

Falciglia, P.P., Malarbì, D. and Vagliasindi, F.G.A., 2016. Removal of mercury from marine sediments by the combined application of a biodegradable non-ionic surfactant and complexing agent in enhanced-electrokinetic treatment. Electrochim Acta 222, 1569-1577.

Gao, P., Wang, S., Cheng, F. and Guo, S., 2022. Improvement of the electrokinetic fluxes by tall fescue: Alleviation of ion attenuation and maintainability of soil colloidal properties. Chemosphere 290, 133128.

Hanay, O., Hasar, H. and Kocer, N.N., 2009. Effect of EDTA as washing solution on removing of heavy metals from sewage sludge by electrokinetic. J Hazard Mater 169(1-3), 703-710.

Huang, R. and Tang, Y., 2015. Speciation Dynamics of Phosphorus during (Hydro)Thermal Treatments of Sewage Sludge. Environ Sci Technol 49(24), 14466-14474.

Kołodyńska, D., Hubicka, H. and Hubicki, Z., 2009. Studies of application of monodisperse anion exchangers in sorption of heavy metal complexes with IDS. Desalination 239(1-3), 216-228.

Kou, Y., Zhao, Q., Cheng, Y., Wu, Y., Dou, W. and Ren, X., 2020. Removal of heavy metals in sludge via joint EDTA-acid treatment: Effects on seed germination. Sci Total Environ 707, 135866.

Li, H., Tian, Y., Liu, W., Long, Y., Ye, J., Li, B., Li, N., Yan, M. and Zhu, C., 2020a. Impact of electrokinetic remediation of heavy metal contamination on antibiotic

628 resistance in soil. Chem Eng J 400, 125866.
629 Li, S., Zeng, W., Jia, Z., Wu, G., Xu, H. and Peng, Y., 2020b. Phosphorus species
630 transformation and recovery without apatite in $FeCl_3$-assisted sewage sludge
631 hydrothermal treatment. Chem Eng J 399, 125735.
632 Liu, H., Basar, I.A., Nzihou, A. and Eskicioglu, C., 2021. Hydrochar derived from
633 municipal sludge through hydrothermal processing: A critical review on its
634 formation, characterization, and valorization. Water Res 199, 117186.
635 Liu, L., Li, W., Song, W. and Guo, M., 2018. Remediation techniques for heavy metal-
636 contaminated soils: Principles and applicability. Sci Total Environ 633, 206-219.
637 Liu, Q., Bai, X., Su, X., Huang, B., Wang, B., Zhang, X., Ruan, X., Cao, W., Xu, Y. and
638 Qian, G., 2020. The promotion effect of biochar on electrochemical degradation
639 of nitrobenzene. J Clean Prod 244, 118890.
640 Liu, Y., Chen, J., Cai, Z., Chen, R., Sun, Q. and Sun, M., 2017. Removal of copper and
641 nickel from municipal sludge using an improved electrokinetic process. Chem
642 Eng J 307, 1008-1016.
643 Ma, D., Su, M., Qian, J., Wang, Q., Meng, F., Ge, X., Ye, Y. and Song, C., 2020. Heavy
644 metal removal from sewage sludge under citric acid and electroosmotic
645 leaching processes. Sep Purif Technol 242, 116822.
646 Moon, D.H., Chang, Y.Y., Lee, M., Koutsospyros, A., Koh, I.H., Ji, W.H. and Park, J.H.,
647 2021. Assessment of soil washing for heavy metal contaminated paddy soil
648 using FeCl3 washing solutions. Environ Geochem Health 43(9), 3343-3350.
649 Peng, G. and Tian, G., 2010. Using electrode electrolytes to enhance electrokinetic
650 removal of heavy metals from electroplating sludge. Chem Eng J 165(2), 388-
651 394.
652 Ping, Q., Lu, X., Li, Y. and Mannina, G., 2020. Effect of complexing agents on
653 phosphorus release from chemical-enhanced phosphorus removal sludge during
654 anaerobic fermentation. Bioresour Technol 301, 122745.
655 Raheem, A., Sikarwar, V.S., He, J., Dastyar, W., Dionysiou, D.D., Wang, W. and Zhao,
656 M., 2018. Opportunities and challenges in sustainable treatment and resource
657 reuse of sewage sludge: A review. Chem Eng J 337, 616-641.
658 Rahman, S., Rahman, I.M.M., Ni, S., Harada, Y., Kasai, S., Nakakubo, K., Begum, Z.A.,
659 Wong, K.H., Mashio, A.S., Ohta, A. and Hasegawa, H., 2022. Enhanced
660 remediation of arsenic-contaminated excavated soil using a binary blend of
661 biodegradable surfactant and chelator. J Hazard Mater 431, 128562.
662 Ryu, B.-G., Park, G.-Y., Yang, J.-W. and Baek, K., 2011. Electrolyte conditioning for
663 electrokinetic remediation of As, Cu, and Pb-contaminated soil. Sep Purif
664 Technol 79(2), 170-176.
665 Song, Y., Ammami, M.T., Benamar, A., Mezazigh, S. and Wang, H., 2016. Effect of
666 EDTA, EDDS, NTA and citric acid on electrokinetic remediation of As, Cd, Cr,
667 Cu, Ni, Pb and Zn contaminated dredged marine sediment. Environ Sci Pollut
668 Res Int 23(11), 10577-10586.
669 Staal, L.B., Petersen, A.B., Jorgensen, C.A., Nielsen, U.G., Nielsen, P.H. and Reitzel,

K., 2019. Extraction and quantification of polyphosphates in activated sludge from waste water treatment plants by ^{31}P NMR spectroscopy. Water Res 157, 346-355.

Suanon, F., Sun, Q., Dimon, B., Mama, D. and Yu, C.P., 2016. Heavy metal removal from sludge with organic chelators: Comparative study of N, N-bis(carboxymethyl) glutamic acid and citric acid. J Environ Manage 166, 341-347.

Tang, J., He, J., Liu, T., Xin, X. and Hu, H., 2017. Removal of heavy metal from sludge by the combined application of a biodegradable biosurfactant and complexing agent in enhanced electrokinetic treatment. Chemosphere 189, 599-608.

Tang, J., He, J., Tang, H., Wang, H., Sima, W., Liang, C. and Qiu, Z., 2020. Heavy metal removal effectiveness, flow direction and speciation variations in the sludge during the biosurfactant-enhanced electrokinetic remediation. Sep Purif Technol 246, 116918.

Tang, J., He, J., Xin, X., Hu, H. and Liu, T., 2018. Biosurfactants enhanced heavy metals removal from sludge in the electrokinetic treatment. Chem Eng J 334, 2579-2592.

Tang, J., Qiu, Z., Tang, H., Wang, H., Sima, W., Liang, C., Liao, Y., Li, Z., Wan, S. and Dong, J., 2021. Coupled with EDDS and approaching anode technique enhanced electrokinetic remediation removal heavy metal from sludge. Environ Pollut 272, 115975.

Tang, Q., Chu, J., Wang, Y., Zhou, T. and Liu, Y., 2016. Characteristics and factors influencing Pb(II) desorption from a Chinese clay by citric acid. Sep Science Technol 51(17), 2734-2743.

Tang, Y., Xie, H., Sun, J., Li, X., Zhang, Y. and Dai, X., 2022. Alkaline thermal hydrolysis of sewage sludge to produce high-quality liquid fertilizer rich in nitrogen-containing plant-growth-promoting nutrients and biostimulants. Water Res 211, 118036.

Temporetti, P., Beamud, G., Nichela, D., Baffico, G. and Pedrozo, F., 2019. The effect of pH on phosphorus sorbed from sediments in a river with a natural pH gradient. Chemosphere 228, 287-299.

Wang, Q., Wang, Z., Awasthi, M.K., Jiang, Y., Li, R., Ren, X., Zhao, J., Shen, F., Wang, M. and Zhang, Z., 2016. Evaluation of medical stone amendment for the reduction of nitrogen loss and bioavailability of heavy metals during pig manure composting. Bioresour Technol 220, 297-304.

Wang, T., Zhai, Y., Zhu, Y., Peng, C., Wang, T., Xu, B., Li, C. and Zeng, G., 2017. Feedwater pH affects phosphorus transformation during hydrothermal carbonization of sewage sludge. Bioresour Technol 245(Pt A), 182-187.

Wang, Y., Han, Z., Li, A. and Cui, C., 2021a. Enhanced electrokinetic remediation of heavy metals contaminated soil by biodegradable complexing agents. Environ Pollut 283, 117111.

Wang, Z., Shen, R., Ji, S., Xie, L. and Zhang, H., 2021b. Effects of biochar derived

712 from sewage sludge and sewage sludge/cotton stalks on the immobilization and
713 phytoavailability of Pb, Cu, and Zn in sandy loam soil. J Hazard Mater 419,
714 126468.
715 Wu, J., Wei, B., Lv, Z. and Fu, Y., 2021a. To improve the performance of focusing
716 phenomenon related to energy consumption and removal efficiency in
717 electrokinetic remediation of Cr-contaminated soil. Sep Purif Technol 272,
718 118882.
719 Wu, Q., Duan, G., Cui, Y. and Sun, J., 2015. Removal of heavy metal species from
720 industrial sludge with the aid of biodegradable iminodisuccinic acid as the
721 chelating ligand. Environ Sci Pollut Res Int 22(2), 1144-1150.
722 Wu, W., Yan, B., Zhong, L., Zhang, R., Guo, X., Cui, X., Lu, W. and Chen, G., 2021b.
723 Combustion ash addition promotes the production of K-enriched biochar and K
724 release characteristics. J Clean Prod 311, 127557.
725 Xia, Y., Tang, Y., Shih, K. and Li, B., 2020. Enhanced phosphorus availability and
726 heavy metal removal by chlorination during sewage sludge pyrolysis. J Hazard
727 Mater 382, 121110.
728 Xu, G., Zhang, Y., Shao, H. and Sun, J., 2016. Pyrolysis temperature affects phosphorus
729 transformation in biochar: Chemical fractionation and ^{31}P NMR analysis. Sci
730 Total Environ 569-570, 65-72.
731 Xu, H., Bai, J., Yang, X., Zhang, C., Yao, M. and Zhao, Y., 2022. Lab scale-study on
732 the efficiency and distribution of energy consumption in chromium
733 contaminated aquifer electrokinetic remediation. Environ Technol Innov 25,
734 102194.
735 Xu, J., Liu, C., Hsu, P.C., Zhao, J., Wu, T., Tang, J., Liu, K. and Cui, Y., 2019.
736 Remediation of heavy metal contaminated soil by asymmetrical alternating
737 current electrochemistry. Nat Commun 10(1), 2440.
738 Xu, Y., Zhang, C., Zhao, M., Rong, H., Zhang, K. and Chen, Q., 2017. Comparison of
739 bioleaching and electrokinetic remediation processes for removal of heavy
740 metals from wastewater treatment sludge. Chemosphere 168, 1152-1157.
741 Yan, W., Chen, Y., Shen, N., Wang, G., Wan, J. and Huang, J., 2021. The influence of a
742 stepwise pH increase on volatile fatty acids production and phosphorus release
743 during Al-waste activated sludge fermentation. Bioresour Technol 320(Pt A),
744 124276.
745 Yesil, H., Molaey, R., Calli, B. and Tugtas, A.E., 2021. Extent of bioleaching and
746 bioavailability reduction of potentially toxic heavy metals from sewage sludge
747 through pH-controlled fermentation. Water Res 201, 117303.
748 Yu, B., Luo, J., Xie, H., Yang, H., Chen, S., Liu, J., Zhang, R. and Li, Y.Y., 2021. Species,
749 fractions, and characterization of phosphorus in sewage sludge: A critical
750 review from the perspective of recovery. Sci Total Environ 786, 147437.
751 Yuan, C. and Weng, C.H., 2006. Electrokinetic enhancement removal of heavy metals
752 from industrial wastewater sludge. Chemosphere 65(1), 88-96.
753 Zeng, Q., Huang, H., Tan, Y., Chen, G. and Hao, T., 2021. Emerging electrochemistry-

based process for sludge treatment and resources recovery: A review. Water Res 209, 117939.
Zhang, L., Mishra, D., Zhang, K., Perdicakis, B., Pernitsky, D. and Lu, Q., 2020. Electrokinetic study of calcium carbonate and magnesium hydroxide particles in lime softening. Water Res 186, 116415.
Zhang, X., Li, J., Fan, W.Y. and Sheng, G.P., 2019. Photomineralization of Effluent Organic Phosphorus to Orthophosphate under Simulated Light Illumination. Environ Sci Technol 53(9), 4997-5004.
Zheng, G., Yu, B., Wang, Y., Ma, C. and Chen, T., 2021. Fate and biodegradation characteristics of triclocarban in wastewater treatment plants and sewage sludge composting processes and risk assessment after entering the ecological environment. J Hazard Mater 412, 125270.
Zheng, X., Liu, T., Guo, M., Li, D., Gou, N., Cao, X., Qiu, X., Li, X., Zhang, Y., Sheng, G., Pan, B., Gu, A.Z. and Li, Z., 2020. Impact of heavy metals on the formation and properties of solvable microbiological products released from activated sludge in biological wastewater treatment. Water Res 179, 115895.